

# Critical exponents of correlated percolation of sites not visited by a random walk

Raz Halifa Levi<sup>1,\*</sup> and Yacov Kantor<sup>2</sup>

<sup>1</sup>The Faculty of Engineering, Tel Aviv University, Tel Aviv 6997801, Israel

<sup>2</sup>School of Physics and Astronomy, Tel Aviv University, Tel Aviv 6997801, Israel

(Dated: May 27, 2024)

We consider a  $d$ -dimensional correlated percolation problem of sites *not* visited by a random walk on a hypercubic lattice  $L^d$  for  $d = 3, 4$  and  $5$ . The length of the random walk is  $\mathcal{N} = uL^d$ . Close to the critical value  $u = u_c$ , many geometrical properties of the problem can be described as powers (critical exponents) of  $u_c - u$ , such as  $\beta$ , which controls the strength of the spanning cluster, and  $\gamma$ , which characterizes the behavior of the mean finite cluster size  $S$ . We show that at  $u_c$  the ratio between the mean mass of the largest cluster  $M_1$  and the mass of the second largest cluster  $M_2$  is independent of  $L$  and can be used to find  $u_c$ . We calculate  $\beta$  from the  $L$ -dependence of  $M_2$  and  $\gamma$  from the finite size scaling of  $S$ . The resulting exponent  $\beta$  remains close to 1 in all dimensions. The exponent  $\gamma$  decreases from  $\approx 3.9$  in  $d = 3$  to  $\approx 1.9$  in  $d = 4$  and  $\approx 1.3$  in  $d = 5$  towards  $\gamma = 1$  expected in  $d = 6$ , which is close to  $\gamma = 4/(d - 2)$ .

## I. INTRODUCTION

Percolation theory [1–3] provides a theoretical framework for several classes of theories describing generation of long-range connectivity from contacts between nearby objects. On regular lattices, these objects are sites or bonds. A group of connected neighboring sites or bonds forms a *cluster*. In this work we consider *site* percolation on hypercubic lattices. Such systems are characterized by a single parameter, such as the probability  $p$  of an occupied sites. A cluster is *spanning* if it contains an uninterrupted path between opposing boundaries in a specific direction. In finite systems of linear size  $L$  the probability  $\Pi(p, L)$  of the existence of such a path gradually increases with increasing  $p$ . For an infinite system  $\Pi(p, \infty)$  becomes a step-function  $\Theta(p - p_c)$  jumping from 0 to 1 at a particular *critical concentration*  $p_c$ . The mean spatial extent (linear size) of *finite* clusters is called the correlation length  $\xi$ . Close to  $p_c$  it diverges as

$$\xi \sim |p - p_c|^{-\nu}. \quad (1)$$

One of the simplest percolation models is Bernoulli site percolation on a  $d$ -dimensional lattice, where each lattice site is *independently* occupied with probability  $p$ . The exponent  $\nu = \nu_B$  of this problem decreases with increasing  $d$  reaching  $\nu_B = \frac{1}{2}$  for  $d \geq d_c = 6$ , i.e., at and above the *upper critical dimension*  $d_c$  [4]. Besides  $\nu$ , the percolation problem is characterized by a large number of additional *critical exponents*, such as  $\gamma$  describing the divergence of the mean finite cluster size  $S$  (an accurate definition will be provided in the Sec. III) in the vicinity of  $p_c$ :

$$S \sim |p - p_c|^{-\gamma}, \quad (2)$$

or the fraction of sites  $P$  belonging to the infinite cluster for  $p > p_c$ , also called the *strength* of the infinite cluster:

$$P \sim (p - p_c)^\beta. \quad (3)$$

For Bernoulli percolation, the values of these and other exponents are known exactly for  $d = 2$  and  $d \geq 6$ , and have accurate numerical estimates for  $d = 3, 4$  and  $5$ . There are numerous equalities relating various exponents describing the behavior close to the threshold, such as the hyperscaling relation

$$d\nu = 2\beta + \gamma \quad (4)$$

and others [1]. As a result, the values of many exponents can be deduced from only two exponents. Nevertheless, due to the limited accuracy of the numerical studies, additional exponents are measured and the values of the results are verified using the known relations.

In Section II we define a correlated percolation model and briefly overview its properties as well as some known results. In Section III we define the main quantities and briefly describe the numerical methods used in this work. Section IV describes the properties of the largest clusters and their use to verify the position of the percolation threshold. Critical exponent  $\beta$  characterizing the strength of the infinite cluster is found from the  $L$ -dependence of the second largest cluster in Section V, while the exponent controlling the behavior of the mean cluster size  $\gamma$  is found in Section VI. Summary Section VII briefly discusses the results.

## II. LONG-RANGE MODEL

Minor modifications of Bernoulli percolation model, such as the introduction of short-range correlations between sites, or consideration of bond percolation, or even power-law correlations  $\sim 1/r^b$  between present sites at distance  $r$  with *large* power  $b$  do not change the critical behavior of the system [5]. However, if  $b < 2/\nu_B$ , then the correlations are relevant, and  $\nu_B$  is replaced [5] by

$$\nu_{\text{long range}} = 2/b. \quad (5)$$

There is a variety of studies of correlated percolation models [6–12]. In this paper, we consider a problem,

\* razhalifa@gmail.com

$d$	$\nu_{\text{th}}$	$\nu_{\text{num}}$	$u_c$	$L_{\text{max}}$
3	2	$2.04 \pm 0.08$	$3.15 \pm 0.01$	512
4	1	$1.0 \pm 0.1$	$2.99 \pm 0.01$	64
5	$\frac{2}{3}$	$0.65 \pm 0.03$	$3.025 \pm 0.008$	32
6	$\frac{1}{2}$	$\sim 0.6$	$3.10 \pm 0.05$	16

TABLE I. Results of previous studies: First two columns show the space dimension  $d$ , and the value of  $\nu$  predicted by Weinrib [5], as applied to our problem [13] in the Eq. (6), respectively. The 3rd and the 4th columns provide numerical estimates of  $\nu$  and  $u_c$  from [13], while the last column gives the maximal linear size of a lattice used in that study.

where an initially full  $d$ -dimensional hypercubic lattice of linear size  $L$  (in lattice constants) and volume  $L^d$  has its sites removed by an  $\mathcal{N}$ -step random walk (RW) on the lattice. The *length* of the RW that starts at a random position is proportional to the *volume* of the lattice, namely  $\mathcal{N} = uL^d$ . Periodic boundary conditions are imposed on the walk on a finite lattice, i.e., the walker exiting through one boundary of the lattice reemerges on the opposite boundary. The parameter  $u$  controls the length of the RW and the fraction  $p$  of unvisited sites. In repeated realizations of this process at fixed  $u$ , the average  $p$  is a monotonically decreasing function of  $u$ . For large  $L$  (and  $d \geq 3$ ) there is a simple relation between these quantities:  $p = \exp(-A_d u)$ , where  $A_d$  are known constants (see Ref. [13] and references therein). An experimental realization of this model involves a gel of crosslinked polymers with the random walker represented by an enzyme that breaks the crosslinks between polymers that it encounters [14, 15] eventually breaking the spanning cluster and turning the solid gel into a liquid. The object of our study is the sites *not visited* by the RW, that represent the surviving crosslinks.

The variable  $u$  naturally replaces  $p$  in this problem, and  $p_c$  is replaced by the critical value  $u_c$ . (Keep in mind that the system percolates, i.e., has spanning clusters of unvisited sites *below*  $u_c$ .) In the previous study, it has been found that on hypercubic lattice for  $3 \leq d \leq 6$  the threshold values  $u_c \approx 3$  [13]. (See Table I.) This problem has been previously studied by Banavar *et al.* in  $d = 2$  and 3 [16], while Abete *et al.* considered the critical behavior near the percolation threshold in  $d = 3$  [17]. More recently Kantor and Kardar studied the percolation properties of the problem for  $2 \leq d \leq 6$  [13], and showed that the problem has no percolation threshold in  $d = 2$  (for more details, see Ref. [18]). While the results of the current study were being summarized in this paper we received a preprint by Chalhoub *et al.* [19] with a detailed numerical study of the critical properties of this problem in large systems in  $d = 3$  and analytical predictions regarding this problem and several similar problems in general  $d$ . We will compare their results with ours wherever it is appropriate.

Figure 1 depicts a typical configuration of the percola-

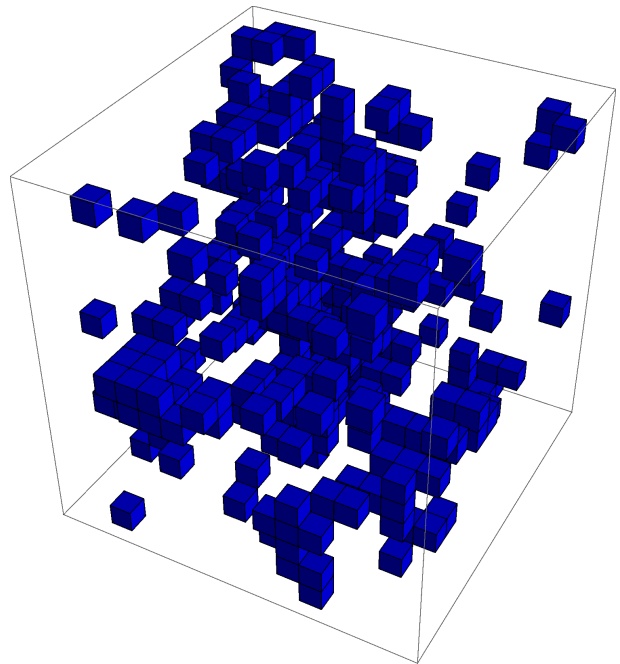


FIG. 1. Three-dimensional percolation in a small system of linear size  $L = 16$ . The sample was created by a random walk of  $\mathcal{N} = uL^3$  steps, where  $u = 4$ . The blue cubes show the *unvisited* sites, which form several clusters. The visited sites form a *single* cluster.

tion of sites (blue cubes) not visited by a RW in  $d = 3$ . In this realization, the number of steps of the RW exceeds four times the number of available lattice positions. Nevertheless, a significant fraction of the sites remains unvisited, since the RW frequently revisits previously visited sites. All *visited* sites form a *single cluster* since they have been created by a single RW. The unvisited sites form many clusters of various sizes. The picture is quite different from the usual geometries of Bernoulli percolation. The RW has a fractal dimension  $\tilde{d}_f = 2$ . On an *infinite* lattice an  $\mathcal{N}$ -step walk explores distance  $r \sim \mathcal{N}^{1/\tilde{d}_f} = \mathcal{N}^{1/2}$ . Within that distance, the density of sites visited by the RW is  $\mathcal{N}/r^d \sim 1/r^{d-2}$ . On a *finite* lattice, a RW walk that exists through one boundary and re-enters through the opposite boundary creates almost uncorrelated strands, and the sites on different strands are no longer power-law correlated. A RW of length  $uL^d$  creates approximately  $uL^{d-2}$  such strands, that contribute to uncorrelated background density of sites. However, at distances  $r$  smaller than the lattice size, there remains a residual correlation of sites that happen to be on the *same* strand of the RW. Consequently, the *cumulant* of the correlation (from which the overall background density has been subtracted) still has  $\sim 1/r^{d-2}$  correlation like a RW on an infinite lattice. Consider a random variable  $v(\vec{x})$  which is 1 if the site at position  $\vec{x}$  is *unvisited* by the RW, and zero otherwise. It is complementary to the variable representing the *visited* site (their sum is 1) and therefore it has the same cumulant:  $\langle v(\vec{x})v(\vec{y}) \rangle_c \sim 1/|\vec{x}-\vec{y}|^{d-2}$  [13].

Thus, the correlation power is  $b = d - 2$ , and the relation (5) becomes

$$\nu = 2/(d - 2), \quad \text{for } 3 \leq d \leq 6. \quad (6)$$

We note that recently Feshanjerdi *et al.* [20] studied a three-dimensional “carbon copy” version of our problem, where they considered percolation of sites *visited* by a RW. Their model is expected to have similar critical properties.

Kantor and Kardar’s study of the problem in  $3 \leq d \leq 6$  [13], focussed on the behavior of the percolation probability  $\Pi(u, L)$  as a function of RW parameter  $u$  and system size  $L$ . As  $L$  increases,  $\Pi(u, L)$  approaches the step function  $\Theta(u_c - u)$ . Thus, by examining the  $u$ -dependence of  $\Pi$  for a sequence of  $L$  values, it was possible to estimate the transition point  $u_c$ , while by studying  $L$ -dependence of the width of the transition between percolating ( $\Pi \approx 1$ ) and non-percolating ( $\Pi \approx 0$ ) states it was possible to determine the exponent  $\nu$ . Table I compares numerically calculated values of  $\nu$  [13] with the predictions of Weinrib [5] in Eq. (6) and provides the calculated values of the thresholds. (In  $d = 3$  an earlier estimate of  $\nu$  on smaller systems ( $L_{\max} = 60$ ) was  $1.8 \pm 0.1$  [17], i.e., it slightly deviated from the predicted value of 2.) The conclusion of [13] was that the numerical results validated the theoretical prediction of Weinrib [5] in  $d = 3, 4$  and 5, and we will use the theoretical values of  $\nu$  in the current work. (Dimension  $d = 6$  is expected to be the upper critical dimension where  $\nu = \frac{1}{2}$  coincides with  $\nu_B$  of Bernoulli percolation. The system sizes in [13] were too small to reliably determine the value of the exponent.)

### III. CLUSTERS AND FINITE SIZE SCALING

In a system of  $N$  sites with  $N_s$  clusters containing  $s$  sites, we define *cluster density*  $n_s \equiv N_s/N$ . The total number of occupied sites on a lattice  $M = \sum_s sN_s$ , and therefore the fraction of occupied sites is  $p = M/N = \sum_s sn_s$ . It is natural to define  $n_s$  and  $p$  as averages over an ensemble of systems, such as  $n_s \equiv \langle N_s \rangle / N$ , where  $\langle \cdot \rangle$  defines ensemble average of “.”. For the simplicity of the notation we will omit the  $\langle \cdot \rangle$  signs where their presence is self-evident from the context. We also consider the thermodynamic limit of infinite lattices  $N \rightarrow \infty$ , where all  $n_s$  and  $p$  approach a finite limit. In an infinite lattice above the percolation threshold  $p_c$ , an infinite cluster is present and occupies some fraction  $P > 0$  of the sites. Since summation over all integer numbers  $s$  does not include an infinite cluster, the  $\sum_s sn_s = p - P$ . (Below the threshold  $P = 0$  and the formula reduces to the expression that we had before.) In finite systems, the distinction between the “would-be-infinite” cluster and other clusters blurs and the transition itself is smeared. Therefore, it is customary [1] in numerical estimates of  $N_s$  on finite lattices to exclude the largest cluster of mass  $s_{\max} \equiv M_1$  of any random realization of the system: For

very large systems above  $p_c$  this is equivalent to the exclusion of the infinite cluster, while below  $p_c$  it slightly decreases the finite cluster size, but this effect decays with increasing  $L$ . Values of  $M_1$  are used to estimate the fraction of the “infinite” cluster  $P = M_1/N$ . This procedure produces a non-vanishing effective  $P$  below the threshold, but its value decays to zero as the system size increases.

In infinite systems, the *second moment*  $\chi \equiv \sum_s s^2 n_s$  characterizes the size (mass) of *finite* cluster, since the sum excludes the infinite cluster, if such is present. In fact the mean size  $S$  of a cluster to which a given occupied site belongs, is given by  $S = \chi/(p - P)$  [1]. (In an infinite system both the mean cluster size  $S$  and the second moment  $\chi$  diverge near  $p_c$  as shown in Eq. (2), and both can be used for numerical estimates of  $\gamma$ .) The expression for  $\chi$  can be re-written as  $\chi = \sum_s s^2 N_s / N = \sum_\alpha s_\alpha^2 / N$ , where the last sum simply represents a sum of squares of sizes of each distinct cluster  $\alpha$  in the system. (In the finite systems in each configuration in our calculations we exclude the largest cluster from that sum.)

For the problem of the sites unvisited by a RW, the system percolates *below*  $u_c$  and in all the expressions describing the behavior of  $S$  and  $P$  the arguments  $p - p_c$  should be replaced by  $u_c - u$ , if the sign of the expression matters.

The second moment  $\chi$  or the mean cluster size  $S$  are the geometrical analogs of the susceptibility in magnetic systems. In an infinite system near the threshold Eq. (2) can be rewritten as  $S \sim |u - u_c|^{-\gamma}$ , and, similarly, Eq. (3) becomes  $P \sim (u_c - u)^\beta$ . The correlation length in Eq. (1) can be rewritten as  $\xi \sim |u - u_c|^{-\nu}$ . In a system of linear size  $L$  the correlation length is naturally truncated by the system size, and consequently  $S$  stops increasing when the expression for diverging  $\xi$  exceeds  $L$ . Similarly,  $P$  which was supposed to vanish at  $u_c$  abandons its power-law decay when  $\xi \sim L$ . In general, a critical quantity  $X$  that was supposed to be singular as  $|u - u_c|^{-x}$ , with either positive or negative exponent  $x$  becomes finite when  $\xi > L$ . It is also possible that the apparent position of the singularity (such as the position of the peak of  $S$ ) may slightly differ from  $u_c$  and can be treated as an “effective percolation threshold”  $u_c^*(L)$ . (Its actual value may depend on the quantity which is being considered.)  $u_c^*(L)$  keeps moving towards  $u_c$  with increasing  $L$ . It is expected that

$$|u_c - u_c^*(L)| \sim L^{-1/\nu}. \quad (7)$$

Finite-size scaling theory was originally developed for thermodynamic systems [21] and later adapted to percolation systems [1]. Since the behavior of the system is controlled by  $\xi/L \sim |u - u_c|^{-\nu}/L$ , it is convenient to describe the system by using parameter  $v = (u - u_c)L^{1/\nu}$ . In terms of  $v$  the position of the peak of  $S$  becomes independent of  $L$ . When  $v$  is small, i.e.,  $|v| < V$ , where  $V$  is some model-dependent number of order unity, the behavior of the system is controlled by the finite size  $L$ , while for  $|v| \gg V$  we expect to recover infinite-system

behavior. In general, the behavior of a critical quantity  $X$  can be described by

$$X = L^{x/\nu} g_X[L^{1/\nu}(u - u_c)] = L^{x/\nu} g_X(v), \quad (8)$$

where  $g_X(v)$  is a scaling function. Thus by drawing  $XL^{-x/\nu}$  vs.  $v$  with properly chosen parameters  $u_c$ ,  $\nu$  and  $x$  it should be possible to collapse all the results into a single curve, which is the function  $g_X(v)$ , as long as both  $L$  and  $\xi$  are significantly larger than the lattice constant. To recover the  $L = \infty$  behavior  $X \sim |u - u_c|^{-x}$ , we must have  $g_X(v) \sim |v|^{-x}$  for  $|v| \gg V$ . For small  $v$  the scaling function approaches some constant  $g_X(0)$  leading to  $u$ -independent result  $X \sim L^{x/\nu}$ .

The numerical procedure used in this work is rather straight-forward: Initially all sites on a hypercubic lattice  $L^d$  are present. The system sizes in  $d = 3$  are  $L = 16, 32, 64, \dots, 512$ . For  $d = 4$  they are  $16, 32, 64$  and  $128$ , while in  $d = 5$  the  $L$ s are increased by approximately factor  $\sqrt{2}$ :  $16, 23, 32, 45$ . These  $L$ s are slightly larger than in the previous study (see Table I). A RW starts at a randomly selected site and for a given  $u$  performs  $uL^d$  steps removing the sites that have been visited. At each realization Hoshen-Kopelman algorithm [22] is used to identify *all* clusters, and from the complete list of clusters all necessary quantities characterizing that configuration can be calculated. For a fixed  $u$  and  $L$  this RW procedure is repeated 1000 times and various quantities are averaged over the realizations. For each  $L$  a sequence of  $u$ s is studied to obtain  $u$ -dependence of such averages at typical steps  $\Delta u = 0.05$ , except for specific situations mentioned in the text.

#### IV. TWO LARGEST CLUSTERS

At any  $d$ , on a finite lattice of linear size  $L$  the typical mass (number of sites)  $M_1$  of the *largest* cluster has a very different  $u$ -dependence than the mass  $M_2$  of the *second largest* cluster: In the percolating region ( $u < u_c$ ),  $M_1$  is essentially the mass of the "would-be-infinite" cluster  $PL^d$ . For a very small  $u$ , we have  $M_1 \approx L^d$  and it decreases with increasing  $u$ . For  $u > u_c$  in the nonpercolating region,  $M_1$  is just the largest of the finite clusters that are present and it keeps decreasing with increasing  $u$ . So overall  $M_1$  is a monotonically decreasing function of  $u$ . For a very small  $u$  almost all space is occupied by the massive spanning cluster, and  $M_2 \approx 1$ . As  $u$  increases (still in the percolating region) so do the sizes of finite clusters and  $M_2$  increases. Above  $u_c$  the typical cluster sizes decrease with increasing  $u$  and so does the mass  $M_2$ . In that region it has a similar behavior to  $M_1$ , but, obviously, is smaller than  $M_1$ . We expect  $M_2$  to have a maximum somewhere around  $u_c$ . Figure 2 shows  $M_1$  and  $M_2$  for several system sizes  $L$  in  $d = 4$ . (Similar behavior is found at other  $d$ s.) Indeed  $M_1$  is a monotonically decreasing function, while  $M_2$  has a maximum at some  $u_c^*(L)$ , which approaches  $u_c$  with increasing  $L$  as in Eq. (7).

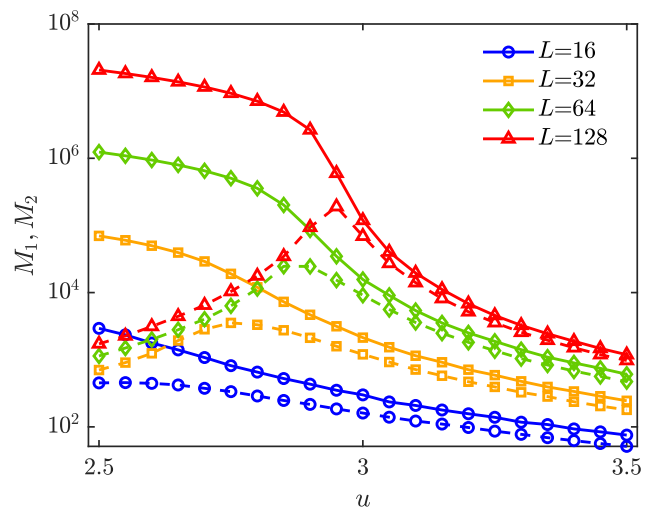


FIG. 2. Semilogarithmic plot of the mean mass  $M_1$  of the largest cluster (solid lines) and the mean mass  $M_2$  of the second largest cluster (dashed lines) as a function of RW parameter  $u$ , in  $d = 4$  for (bottom to top)  $L = 16$  (blue circles),  $32$  (yellow squares),  $64$  (green diamonds) and  $128$  (red triangles). Here, as in other graphs, each point represents an average over 1000 configurations. Relative statistical errors in  $M_1$  and  $M_2$  are  $\lesssim 4\%$ , which on logarithmic scale results in error bars  $\Delta \log_{10} M_2 \lesssim 0.02$  which are smaller than the symbol sizes. Horizontal separation between data points  $\Delta u = 0.05$ . Qualitatively similar behavior was observed in  $d = 3$  and  $d = 5$ .

At the percolation threshold, the largest cluster has fractal structure, and its mass increases with the system size as  $M_1 \sim L^{d_f}$  [1], where  $d_f$  is the fractal dimension of the infinite cluster. However, it has been known for quite some time [23–25] that for Bernoulli percolation at the threshold the mass of the *second* largest cluster  $M_2$  (as well as 3rd and higher rank clusters) also scales with the same power, although it has a smaller prefactor. Therefore, one can expect that the *ratios* of two such cluster masses, represented either by the ensemble average  $\langle M_1/M_2 \rangle$ , or by  $\langle M_1 \rangle / \langle M_2 \rangle$  will scale with 0th power of  $L$ . So this ratio can be treated using the same finite size arguments that were used for  $X$  and lead to scaling form (8), with  $x = 0$  and a different scaling function [26]  $g_0$ . While this reasoning originally applied to Bernoulli percolation, it originates from the argument that at a critical point in the absence of length scale both the largest and the second largest clusters share the same behavior. Therefore this property can be expected (subject to verification) in our correlated percolation problem. In such a case we expect

$$\langle M_1/M_2 \rangle \text{ or } \langle M_1 \rangle / \langle M_2 \rangle = g_0[L^{1/\nu}(u - u_c)] = g_0(v). \quad (9)$$

At  $u = u_c$  this equation means that the ratio of masses of the first and the second largest clusters at the critical point should be  $g_0(0)$ , i.e., independent of  $L$ . The presence of such an intersection at  $u_c$  both confirms that the first and the second largest clusters have the same frac-

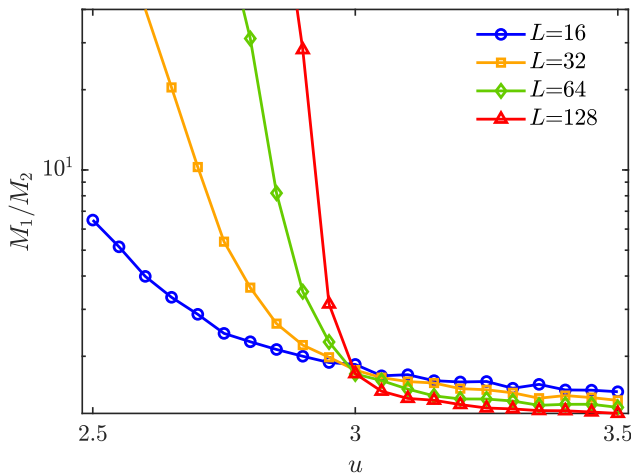


FIG. 3. Semilogarithmic plot of the ratios of mean mass  $M_1$  of the largest cluster and the mean mass  $M_2$  of the second largest cluster as a function of RW length parameter  $u$  in  $d = 4$  for system sizes (left to right on the top parts of the graphs)  $L = 16$  (blue circles),  $32$  (yellow squares),  $64$  (green diamonds) and  $128$  (red triangles). This Figure uses the same data as Fig. 2, and shares the same technical details. The intersection points of subsequent- $L$  lines are between  $2.99$  and  $3.00$  and provide an estimate for  $u_c$  (Smaller  $\Delta u$ s were used close to  $u_c$  but the extra data points are not shown here.) Qualitatively similar behavior was observed in  $d = 3$  and  $d = 5$ .

tal dimension, and enables an alternative approach for an accurate determination of the percolation threshold. This method has been successfully used by da Silva *et al.* [27] to locate  $p_c$  in Bernoulli percolation problem.

The study in Ref. [13] of correlated percolation extracted the value of  $u_c$  by examining the percolation probability  $\Pi(u, L)$  as a function of  $u$  for several values of  $L$ , and observing the approach of that function to the infinite- $L$  limit of step function  $\Theta(u_c - u)$ . With increasing  $u$  the function  $\Pi(u, L)$  monotonically decreases from a percolating small- $u$  regime to a nonpercolating large- $u$  region. The effective transition point  $\tilde{u}$  was defined as a point where  $\Pi(\tilde{u}, L) = c$ , with an arbitrary constant  $0 < c < 1$ . Clearly, the value of  $\tilde{u}$  depends both on  $L$  and  $c$ . Since in the  $L \rightarrow \infty$  limit the  $\Pi$  becomes a step function, in that limit  $\tilde{u} \rightarrow u_c$  independently of the choice of  $c$ . Indeed, in Ref. [13] it has been shown that various choices of  $c$  lead to similar  $L \rightarrow \infty$  extrapolations. However, all  $\tilde{u}$  values exhibited significant  $L$ -dependence, and therefore it is beneficial to use an alternative method to confirm that threshold values appearing in Table I. We apply the method of da Silva *et al.* [27] to our problem. Figure 3 depicts the  $u$ -dependence of  $M_1/M_2$  for various values of  $L$  in  $d = 4$ . We note that the intersection points between various lines are concentrated between  $2.99$  and  $3.00$  even for moderate  $L$ s. This verifies the value  $u_c = 2.99 \pm 0.01$  that has been obtained by strong extrapolations in Ref. [13].

We performed similar studies of  $M_1/M_2$  in  $d = 3$  and  $d = 5$  and confirmed the known values of  $u_c$  listed in Table I. (Fig. 1 in Ref. [19] uses an analogous method of line-intersection for different types of quantities to determine  $u_c$  in  $d = 3$  and concludes that our original value  $u_c = 3.15$  was correct.) We will use the  $u_c$  values from Table I in the remainder of this article. While the results obtained in the following sections require the knowledge of  $u_c$ , they are rather insensitive to its exact value and even changes in the values of  $u_c$  as large as  $0.01$  or  $0.02$  do not modify the estimates of the critical exponents.

## V. EXPONENT $\beta$

Critical exponent  $\beta$  is defined by the behavior of the infinite cluster  $P$  near the percolation threshold, i.e., in an infinite system  $P \sim (u_c - u)^\beta$ , for  $u < u_c$ . One can directly plot measured  $P$  vs.  $u_c - u$  on a logarithmic plot for a sequence of increasing  $L$ s, and determine the exponent  $\beta$ . For a finite  $L$  the power-law is truncated when  $\xi$  reaches  $L$ , it is possible to treat that truncation more systematically, by considering a finite size scaling form for  $P$  which is analogous to Eq. (8)

$$P = L^{-\beta/\nu} g_P[L^{1/\nu}(u - u_c)] = L^{-\beta/\nu} g_P(v), \quad (10)$$

where  $g_P(v)$  is a scaling function, which for large *negative*  $v$  should have the behavior  $g_P(v) \sim (-v)^\beta$ , in order to recover the desired  $L$ -independent behavior of  $P$ , while for small  $v$  we obtain  $u$ -independent result  $P \sim L^{-\beta/\nu}$ . Since  $P$  is small close to  $u_c$  it increases the relative statistical errors and reduces the accuracy of the numerical calculations near that point. On the other hand, one can concentrate on a fixed  $v$ , such as  $v = 0$ , and explore the relation  $P = L^{-\beta/\nu} g_P(0)$ . Since  $P = M_1/L^d$ , we may use the relation  $M_1 \sim L^{d_f}$ , with the fractal dimension

$$d_f = d - \beta/\nu. \quad (11)$$

The direct measurement of the fractal dimension of  $M_1$  is problematic, since this quantity decreases fast (for large  $L$ ) near  $u_c$  (or  $v = 0$ ) as can be seen in Fig. 2. However,  $M_2$  does *not* have this deficiency, and simply has a maximum for small negative  $v = v_{\max}$ . Thus by plotting  $M_2(v = 0)$  as a function of  $L$  on a logarithmic scale one can determine  $d_f$ , and, consequently, the exponent  $\beta$ .

Solid lines in Fig 4 depict on a logarithmic scale the dependence of  $M_2$  at  $u_c$  on system size  $L$ , in the complete range of  $L$ s used for each  $d = 3, 4$  and  $5$ . From the slope of the lines ( $d_f$ ) and from Eq. (11) we deduce  $\beta = 0.98 \pm 0.04$  in  $d = 3$ ,  $\beta = 1.00 \pm 0.06$  in  $d = 4$ , and  $\beta = 1.09 \pm 0.05$  in  $d = 5$ . The stated errors combine small statistical errors of individual  $M_2$  data points (relative errors smaller than 4%) with the scatter of the points around the straight line. We could not determine a systematic  $L$ -dependence of the slope, which might indicate that we are measuring an effective exponent which

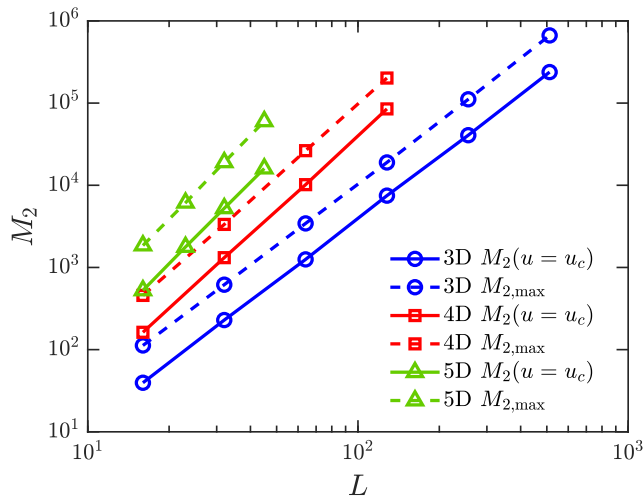


FIG. 4. Logarithmic plots of the mean mass  $M_2$  of the *second* largest cluster measured at  $u_c$  ( $v = 0$ ) (solid lines) or at the maximum of the curve ( $v = v_{\max}$ ) (dashed lines) as a function of  $L$  for (bottom to top pairs of lines)  $d = 3$  (blue circles),  $d = 4$  (red squares) and  $d = 5$  (green triangles). Each data point depicts an ensemble average and the error bars, as explained in Fig. 2, are smaller than the symbol sizes. Slopes of the curves are the fractal dimensions  $d_f$  of the second largest clusters.

changes with increasing  $L$ . If such a change was present, it was masked by the statistical fluctuations of the slope.

The result for  $d = 3$  should be compared with the result  $\beta = 1.0 \pm 0.1$  of Abete [17] obtained on smaller systems ( $L_{\max} = 60$ ). (In that calculation a slightly smaller value of  $\nu$  was used.) Our result in  $d = 3$  is also consistent (within quoted errors) with the result obtained in Ref. [19] for larger systems ( $L_{\max} = 600$ ). Similar result was also obtained by Feshanjerdi *et al.* [20] for a problem of *visited* sites; they conjectured that the exact value of  $\beta$  in  $d = 3$  should be the integer value 1.

As an additional check of the presence or absence of systematic errors, we measured  $M_2$  at its maximal value. We verified that, within statistical uncertainty, the maximal values of  $M_2$  for all  $L$  appear at the same value of  $v_{\max}$ . This is correct for each  $d$ , although the actual definition of  $v$  depends on  $d$  since it involves specific  $u_c$  and  $\nu$ . Thus, the measurement of  $M_2(v = v_{\max})$  for various  $L$ s should produce the same  $L$ -dependence  $M_2 \sim L^{d_f}$ , although with a larger prefactor, as we got for  $v = 0$  (or  $u = u_c$ ). This method of measurement introduces an additional source of errors, since finding maximal  $M_2$  requires interpolation between data points close to that maximum. The presence of this additional error increase in the estimated statistical errors. Dotted lines in Fig. 4 depict  $M_2$  as a function of  $L$  measured at the points of maxima. The measured slopes ( $d_f$ ) produce slightly different values:  $\beta = 0.99 \pm 0.07$  in  $d = 3$ ,  $\beta = 1.07 \pm 0.06$  in  $d = 4$ , and  $\beta = 1.13 \pm 0.05$  in  $d = 5$ . While the results at  $v = v_{\max}$  are less reliable, they are similar to the previous set of  $\beta$ s.

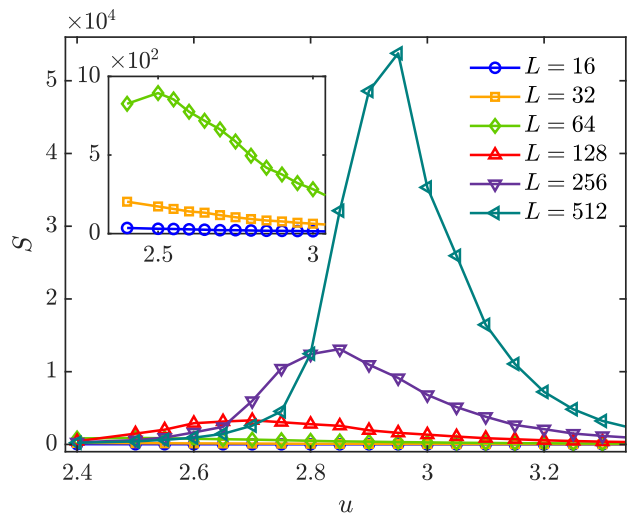


FIG. 5. Mean cluster size  $S$  vs.  $u$  in  $d = 3$  for  $L = 16, 32, \dots, 512$ . Error bars are smaller than the symbols. The inset shows the graphs for the three smallest  $L$ s with an expanded vertical scale. The expected critical point is  $u_c = 3.15$ , while the maxima of the curves appear at slightly lower values  $u_c^*(L)$  that drift towards  $u_c$  with increasing  $L$ .

As mentioned at the beginning of this section, the behavior of  $g_P(v)$  for *large* negative  $v$  is consistent with the expected power-law but is not accurate enough to determine the value of  $\beta$ .

We note, that in  $d = 6$  the exponent of our problem should coincide with the exponent of Bernoulli percolation and have mean field value  $\beta = 1$ . The fact that  $\beta$  maintains the value so close to 1 in all dimensions makes one wonder if  $\beta = 1$  is the exact dimension-independent value of  $\beta$ . Such conjecture has been made by Feshanjerdi *et al.* [20] in  $d = 3$  (for a system of visited sites) and theoretically suggested to be valid in other dimensions by Chalhoub *et al.* [19] (see Table I in their work).

## VI. EXPONENT $\gamma$

Mean cluster size  $S$  is one of the most important characteristics of percolation. In infinite systems, similarly to the susceptibility in magnetic systems, it diverges at the critical point as in Eq. (2), and it would be possible to measure the exponent  $\gamma$  by directly plotting  $S$  as a function of the distance from the critical point on a logarithmic scale. (Exponent  $\gamma$  is expected to be the same both above and below that point.) However, in a finite system, the divergence is truncated when  $\xi$  exceeds  $L$ . Figure 5 depicts  $S$  measured in  $d = 3$  as a function of  $u$  for system sizes  $L$  ranging from 16 to 512. As  $L$  increases, the height of the peak in  $S$  increases approximately as  $L^2$ . The position of the peak appears at some  $u_c^*(L)$ , which is smaller than  $u_c$  and this effective critical point shifts towards  $u_c$  with increasing  $L$  as indicated by

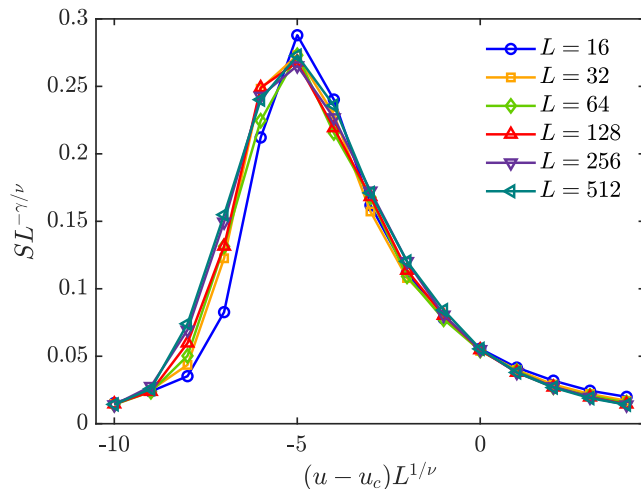


FIG. 6. Data-collapse plot of the scaled mean cluster size  $SL^{-y}$  in  $d = 3$  vs. scaled parameter  $v = (u - u_c)L^{1/\nu}$ . This graph was obtained for  $\gamma = y\nu = 3.90$  and it remains a good fit when  $\gamma$  is changed by  $\pm 0.05$ . This graph is a scaled form of Fig. 5. The error bars are smaller than the sizes of the symbols.

Eq. (7), while the height of the peak increases almost as  $L^2$ . As with other critical quantities, we will use scaled variable  $v = (u - u_c)L^{1/\nu}$  and describe the behavior of  $S$  using scaling form analogous to Eq. (8), namely

$$S = L^{\gamma/\nu} g_S[L^{1/\nu}(u - u_c)] = L^{\gamma/\nu} g_S(v), \quad (12)$$

where  $g_S(v)$  is a scaling function. To recover the  $L = \infty$  behavior  $S \sim |u - u_c|^{-\gamma}$ , we must have  $g_S(v) \sim |v|^{-\gamma}$  for  $|v| \gg V$ . For small  $v$  the scaling function approaches some constant  $g_S(0)$  leading to  $u$ -independent result  $S \sim L^{\gamma/\nu}$ . Instead of focussing on  $v = 0$ , we can look at a point  $v = v_{\max}$ , where all  $S$  reach their maxima independently of  $L$ . At this point, we also expect  $S \sim L^{\gamma/\nu}$  but with a larger prefactor. In fact, the exponent  $\gamma$  can be determined from the entire function  $g_S(v)$ : We need to plot  $SL^{-\gamma/\nu}$  vs.  $v$ . Such a plot should produce the function  $g_S(v)$ . The graphs for several  $L$ s should collapse into a single plot, provided the fitting parameter  $y \equiv \gamma/\nu$  has been properly selected. In general, we should use three fit parameters  $\gamma$ ,  $\nu$  and  $u_c$ . However, the latter two are well known to us, - see Table I. (The fitting is insensitive to small changes in  $u_c$ .) We therefore, use the known values of  $\nu = \nu_{\text{th}} = 2$  and  $u_c = 3.15$  from Table I and adjust only the parameter  $y$  that depends on  $\gamma$ . Using the above values, Fig. 6 presents the same results as Fig. 5 in a scaled form where the horizontal axis uses variable  $v = (u - u_c)L^{1/\nu}$ . The vertical axis represents the scaled cluster size  $SL^{-y}$ , with the fit parameter  $y$  corresponding to  $\gamma = 3.90$ . The fit remains good up to a shift of  $\pm 0.05$  in  $\gamma$ . To ensure an easy comparison between graphs for different  $L$ s, we replaced steps  $\Delta u = 0.05$  between data points by steps  $\Delta v = 1$ , i.e., in terms of  $\Delta u$  the size of the steps changed with  $L$ . Note, that the best-fit value of  $y$  is very close

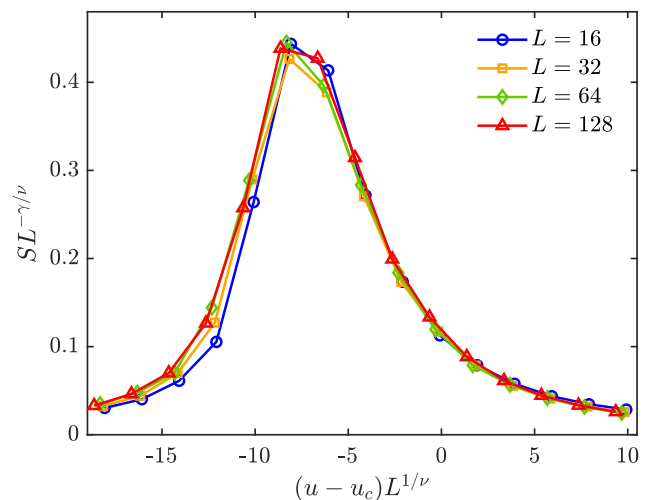


FIG. 7. Data-collapse plot of the scaled mean cluster size  $SL^{-y}$  in  $d = 4$  vs. scaled parameter  $v = (u - u_c)L^{1/\nu}$ . It is analogous to  $d = 3$  graph in Fig. 6. The exponent  $y$  was adjusted to get the best data collapse. This graph was obtained for  $\gamma = y\nu = 1.90$  and it remains a good fit when  $\gamma$  is changed by  $\pm 0.05$ . (Value of  $u_c = 2.995$  was used in this fit.) The error bars are smaller than the symbol sizes.

to 2. The obtained value of  $\gamma$  should be compared with  $\gamma \approx 3.5$  by Abete *et al.* [17] obtained on smaller systems ( $L_{\max} = 60$ ) and with a slightly smaller numerical value of  $\nu$ , and  $\gamma \approx 4.0$  obtained by Chalhoub *et al.* [19] on a slightly larger system.

Our result was extracted from the behavior for small  $v$  behavior of  $g_S(v)$ . As expected, for large  $|v|$  we observe a power law which is consistent with  $|v|^{-\gamma}$ , but the quality and the range of the data is too small for an accurate determination of the power.

We repeated the above calculations in  $d = 4$  and  $d = 5$ . As before we opted for steps  $\Delta v = 1$  and used  $u_c$  and  $\nu$  from Table I. The decreasing range of  $L$  leads to decreasing reliability of the fit. As an example, we present Fig. 7 that shows the scaled results in  $d = 4$ , for  $L$  ranging from 16 to 128. By fitting  $y$  we find  $\gamma = 1.90 \pm 0.05$ , and again parameter  $y$  is very close to 2. Similar analysis was performed in  $d = 5$  on systems of even smaller linear size  $L$  ranging from 16 to 45. The collapse plot (not shown) has slightly lower quality and the best fit leads to the estimate  $\gamma = 1.30 \pm 0.05$ .

As in the three-dimensional case we compared the values of  $\gamma$  obtained for small values of  $v$  with possible power law behavior  $|v|^{-\gamma}$ . Again, we obtained a reasonable correspondence for large negative values of  $v$ , although the accuracy of those results was much lower. (We did not see a clear power law for large positive  $v$ .)

We expect the exponents  $\beta$  obtained in the previous section and the exponents  $\gamma$  obtained in this section to satisfy the hyperscaling relation (4). Indeed by inserting the calculated values the relation is approximately satisfied if we allow for errors in the exponents. In fact, we

can use (4) in an opposite way: if we substitute  $\beta = 1$  into the equation, and use  $\nu$  from (6) we find that in our problem

$$\gamma = 4/(d - 2) . \quad (13)$$

We can see that this expression is very close to the values of  $\gamma$  obtained in all dimensions. (We also note that (13) leads for all  $3 \leq d \leq 6$  to the exponent  $y = \gamma/\nu = 2$ .)

## VII. DISCUSSION

The problem of sites not visited by a RW presents a relatively simple case of correlated percolation. In this work we calculated exponents  $\beta$  and  $\gamma$  in  $d = 3, 4$  and  $5$ , with reasonable accuracy, using system sizes comparable with the previous works. (There were no previous results in  $d = 4$  and  $5$ .) We used different methods to measure the exponents: measurement of the fractal dimension of the second largest cluster for calculation of  $\beta$  and finite size scaling for  $\gamma$ . Our results hint at simple numerical values for the critical exponents, and one may hope to derive these values from simple geometrical considerations.

- 
- [1] D. Stauffer and A. Aharony, *Introduction to Percolation Theory*, 2nd ed. (Taylor and Francis, London, UK, 1991).
- [2] G. Gremmett, *Percolation*, 2nd ed. (Springer, Berlin, 1999).
- [3] A. A. Saberi, Recent advances in percolation theory and its applications, *Phys. Rep.* **578**, 1 (2015).
- [4] G. Toulouse, Perspectives from the theory of phase transitions, *Il Nuovo Cimento B* **23**, 234 (1974).
- [5] A. Weinrib, Long-range correlated percolation, *Phys. Rev. B* **29**, 387 (1984).
- [6] A. Coniglio and A. Fierro, Correlated percolation, in *Encyclopedia of Complexity and Systems Science*, part 3 (Springer, New York, 2009) pp. 1596–1615.
- [7] G. Gori, M. Michelangeli, N. Defenu, and A. Trombettoni, One-dimensional long-range percolation: A numerical study, *Phys. Rev. E* **96**, 012108 (2017).
- [8] O. Riordan and L. Warnke, Explosive percolation is continuous, *Science* **333**, 322 (2011).
- [9] R. M. D’Souza and J. Nagler, Anomalous critical and supercritical phenomena in explosive percolation, *Nat. Phys.* **11**, 531 (2015).
- [10] Y. Kantor, Three-dimensional percolation with removed lines of sites, *Phys. Rev. B* **33**, 3522 (1986).
- [11] K. J. Schrenk, N. Posé, J. J. Kranz, L. V. M. van Kessenich, N. A. M. Araujo, and H. J. Herrmann, Percolation with long-range correlated disorder, *Phys. Rev. E* **88**, 052102 (2013).
- [12] K. J. Schrenk, M. R. Hilário, V. Sidoravicius, N. A. M. Araújo, H. J. Herrmann, M. Thielmann, and A. Teixeira, Critical fragmentation properties of random drilling: how many holes need to be drilled to collapse a wooden cube?, *Phys. Rev. Lett.* **116**, 055701 (2016).
- [13] Y. Kantor and M. Kardar, Percolation of sites not removed by a random walker in  $d$  dimensions, *Phys. Rev. E* **100**, 022125 (2019).
- [14] H. Berry, J. Pelta, D. Lairez, and V. Larreta-Garde, Gel-sol transition can describe the proteolysis of extracellular matrix gels, *Biochim. Biophys. Acta* **1524**, 110 (2000).
- [15] G. C. Fadda, D. Lairez, B. Arrio, J.-P. Carton, and V. Larreta-Garde, Enzyme-catalyzed gel proteolysis: an anomalous diffusion-controlled mechanism, *Biophys. J.* **85**, 2808 (2003).
- [16] J. R. Banavar, M. Muthukumar, and J. F. Willemsen, Fractal geometries in decay models, *J. Phys. A: Math. Gen.* **18**, 61 (1985).
- [17] T. Abete, A. de Candia, D. Lairez, and A. Coniglio, Percolation model for enzyme gel degradation, *Phys. Rev. Lett.* **93**, 228301 (2004).
- [18] A. Federbush and Y. Kantor, Percolation perspective on sites not visited by a random walk in two dimensions, *Phys. Rev. E* **103**, 032137 (2021).
- [19] C. Chalhoub, A. Drewitz, A. Prévost, and P.-F. Rodriguez, Universality classes for percolation models with long-range correlations, *ArXiv:2403.18787* (2024).
- [20] M. Feshanjerdi, A. A. Masoudi, P. Grassberger, and M. Ebrahimi, Aftermath epidemics: Percolation on the sites visited by generalized random walk, *Phys. Rev. E* **108**, 024312 (2023).
- [21] V. Privman and M. E. Fisher, Universal critical amplitudes in finite-size scaling, *Phys. Rev. B* **30**, 322 (1984).
- [22] J. Hoshen and R. Kopelman, Percolation and cluster distribution. I. Cluster multiple labeling technique and critical concentration algorithm, *Phys. Rev. B* **14**, 3438 (1976).
- [23] A. Margolina, H. J. Herrmann, and D. Stauffer, Size of largest and second largest cluster in random percolation, *Phys. Lett. A* **93**, 73 (1982).
- [24] N. Jan, D. Stauffer, and A. Aharony, An infinite number of effectively infinite clusters in critical percolation, *J. Stat. Phys.* **92**, 325 (1998).
- [25] N. Jan, Large lattice random site percolation, *Physica A* **266**, 72 (1999).
- [26] C. R. da Silva, M. L. Lyra, and G. M. Viswanathan, Boundary condition dependence of cluster size ratios in random percolation, *Int. J. Mod. Phys. C* **11**, 1411 (2000).
- [27] C. R. da Silva, M. L. Lyra, and G. M. Viswanathan, Largest and second largest cluster statistics at the percolation threshold of hypercubic lattices, *Phys. Rev. E* **66**, 056107 (2002).